New paradigm for imaging systems

W. Thomas Cathey and Edward R. Dowski

We describe a new paradigm for designing hybrid imaging systems. These imaging systems use optics with a special aspheric surface to code the image so that the point-spread function or the modulation transfer function has specified characteristics. Signal processing then decodes the detected image. The coding can be done so that the depth of focus can be extended. This allows the manufacturing tolerance to be reduced, focus-related aberrations to be controlled, and imaging systems to be constructed with only one optical element plus some signal processing.

OCIS codes: 080.3620, 110.0110, 110.2990, 110.0180, 110.4850, 180.0180.

1. Introduction and Background

The new paradigm that we describe for the design of imaging systems has been termed wave-front coding. These coded optical systems are arrived at by means of designing the coding optics and the signal processing as an integrated imaging system. The results are imaging systems with previously unobtainable imaging modalities and require a modification of the optics for coding the wave in the aperture stop or an image of the aperture stop. This coding produces an intermediate image formed by the optical portion of the system that gathers the image. Signal processing is then required for decoding the intermediate image to produce a final image. The coding can be designed to make the imaging system invariant to certain parameters or to optimize the imaging system's sensitivity to those parameters. One example is the use of image coding to preserve misfocus (and hence, range or distance) information. Another example is the use of different types of codes to make the image invariant to misfocus. These new focus-invariant imaging systems can have more than an order of magnitude increase in the depth of field. Our emphasis in this paper is on the use of the increased depth of focus to design new types of imaging systems. An example of the new imaging systems that can be constructed is a single-element lens that has a small $F/\#$, wide field of view, and diffraction-limited imaging. It also can have greatly relaxed assembly tolerances, because of its invariance to focus-related aberrations.

Coding of signals for optimally conveying particular information is not new. In radar the transmitted pulses are coded for optimally providing information concerning a target's range, for example. The appropriate signal processing to extract the range information is designed in conjunction with the transmitted signal. The integrated design of the optical image-gathering portion along with the signal processing normally is not done in the design of imaging systems. There are exceptions such as tomography, coded aperture imaging, and sometimes, interferometric imaging. In 1984 a group that was investigating the limits of resolution pointed out the potential of increasing the performance of imaging systems by jointly designing the optics and the signal processing.[1]

There have been several descriptions of ways to increase the depth of field of imaging systems. These include the research of Ojeda-Castañeda *et al.*[2] that described attenuating apodizers to block portions of the aperture to extend the depth of field. Also, the depth of field is slightly greater in lenses that have spherical aberration. In both these cases, the wave front is modified, in one case by means of changing the wave amplitude and in the other by a deviation from the traditional ideal phase front. However, in both cases, the increase in the depth of field is only a few percent. Häusler extended the depth of field by requiring that the focus be continuously changed during the exposure time of the camera.[3] This resulted in a modulation transfer function (MTF) for the imaging system that was the

W. T. Cathey (cathey@colorado.edu) is with the Department of Electrical and Computer Engineering, University of Colorado, Boulder, Boulder, Colorado 80309-0425. E. R. Dowski is with CDM Optics, Incorporated, 4001 Discovery Drive, Suite 2110, Boulder, Colorado 80303-7816.

Received 15 January 2002; revised manuscript received 13 June 2002.

0003-6935/02/296080-13$15.00/0

© 2002 Optical Society of America

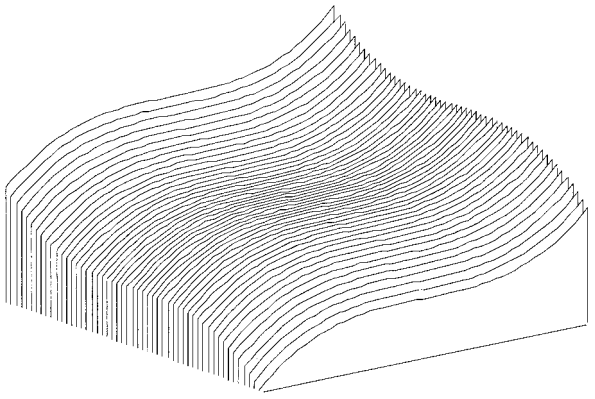

Fig. 1. Rectangularly separable cubic phase surface described by Eq. (1).

incoherent superposition of the MTFs for the different foci during the exposure. To form an acceptable image, signal processing was used.

We first show how the new paradigm is used to increase the depth of focus of an imaging system and give examples of how the improved system can be used. We then review the theory behind wave-front coding. The analysis and design tools are described that are useful in creating systems with coded images. Examples are given of imaging systems that have been designed with this new paradigm, including a simple lens for infrared (IR) operation over a wide temperature range and a single-element high-performance lens. Trade-offs are discussed, and examples are given in which performance is traded for simplicity and speed of processing. Other examples show the trade-offs between the amount of the extension of the depth of focus and the increase in the noise that is due to the additional signal processing.

2. Hybrid Optical–Digital Imaging Systems and Examples of Unique Capabilities

To code the image or wave front in these hybrid imaging systems, the optics in the image-gathering portion of the system are modified in order to change the point-spread function (PSF) of the system. Because the PSF is modified, the image from the optics appears to be degraded and is termed the intermediate image. Signal processing must then be used to decode the image and obtain a high-quality image that has preserved the aspects of the object that are of most interest. Range is one example of an object aspect that can be preserved in a manner that will make its retrieval possible with a hybrid system.[4,5] Such application is not discussed in this paper. Attention here is restricted to extending the depth of focus of the imaging system and to what types of imaging systems can be designed.

If an optical surface with the form mathematically described by

$$z = \alpha(x^3 + y^3) \tag{1}$$

and shown in Fig. 1 is placed in the aperture stop, or if that form is added to the surface of an existing lens near the aperture stop, the depth of focus is extended.[6] Figure 2 shows the effect of a one-dimensional cubic phase surface on an ideal one-dimensional lens. Note that the rays do not focus as in the case of a normal lens but form an extended bundle in the re-

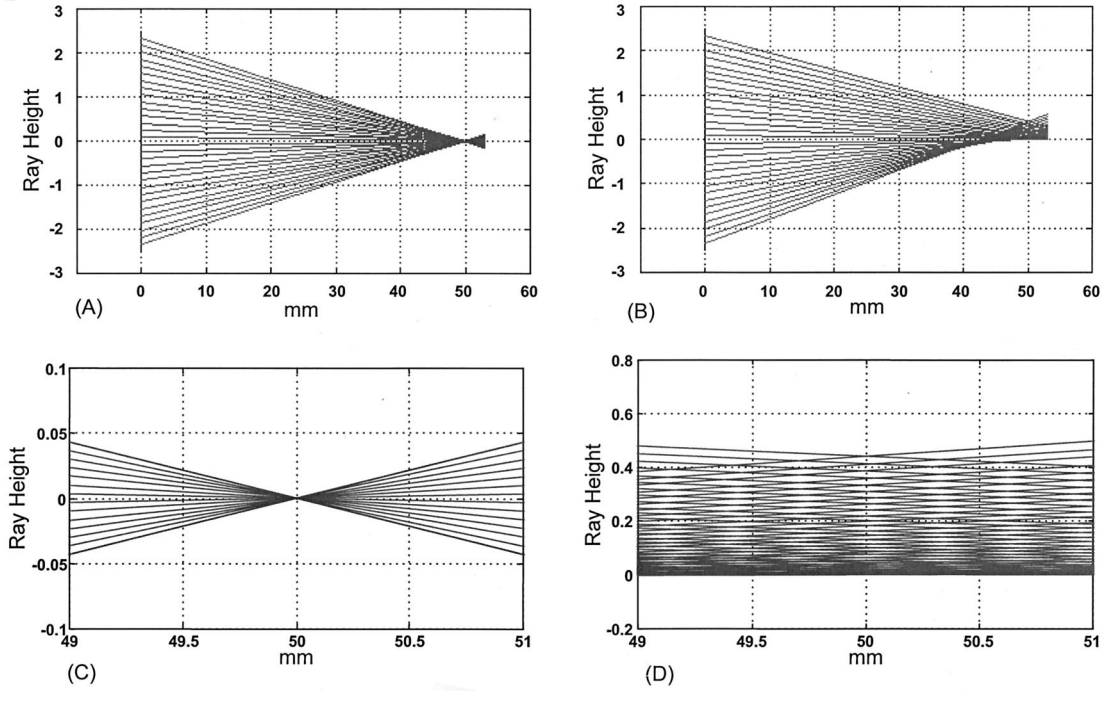

Fig. 2. Rays of a point source focused by a one-dimensional lens (A) without and (B) with a cubic phase plate of Eq. (1) incorporated. The detail near the normal image plane is shown in (C) and (D).

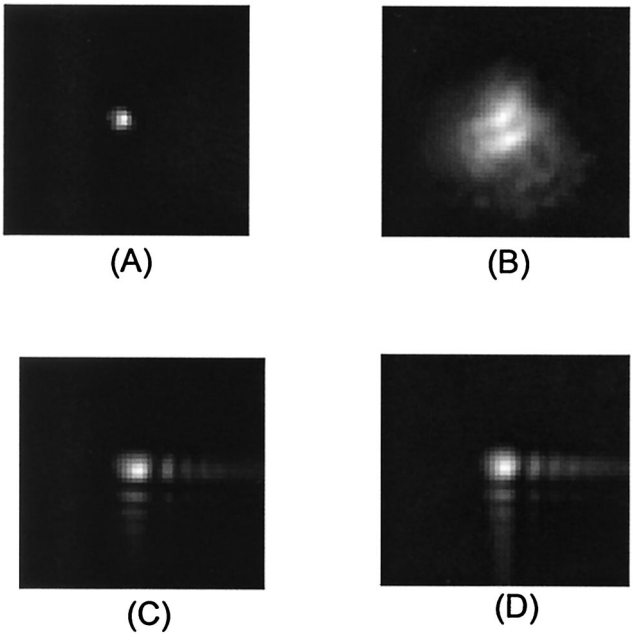

Fig. 3. PSFs associated with the rays of Fig. 2. The PSFs for a normal system are shown for (A) in focus and (B) out of focus. The PSFs for a coded system are shown (C) in the normal region of focus and (D) in the out-of-focus region.

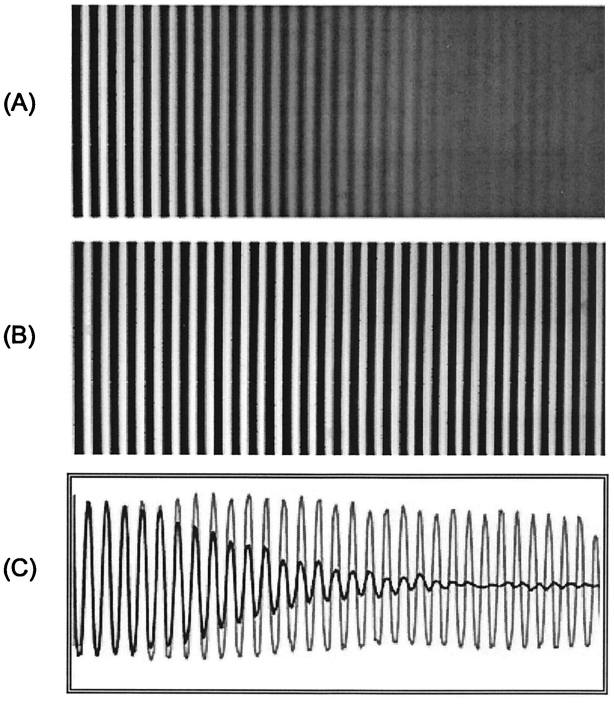

Fig. 4. Image of a bar pattern that was tilted at 60° to the image plane. (A) Image from a conventional system, (B) image from a coded system after signal processing, and (C) traces through both images.

gion of the image plane. Cross sections of the bundle of rays show that the PSF of the imaging system does not change over a large region. The two-dimensional PSFs are shown in Fig. 3. An image formed with a coded PSF appears blurred because of the large extent of the PSF. However, the image has the same blur throughout the depth of the image. Experimentally acquired images of a tilted bar pattern are shown in Fig. 4, where the bar is tilted at 60° to the focal plane. The image from a conventional system is seen to go so far out of focus that there is a contrast reversal in the image. The intermediate coded image from the hybrid system has the same blur throughout, and after processing, the entire image is sharp and clear.

To form the final image, the coded image must be decoded with signal processing. This can be done by use of the PSF to deconvolve the intermediate image and obtain the final image. Because the PSF does not appreciably change over a large region of misfocus, the same digital filter can be used no matter what the misfocus would be in the conventional system. Figure 5 shows the Fourier transform of the PSFs of Fig. 3, which produces the optical transfer functions or OTFs. Figure 5 shows that the MTF (the magnitude of the OTF) of the conventional system varies dramatically with misfocus and that with a large misfocus, zeros appear in the MTF. Each misfocus value results in a different MTF and in zeros in different locations. Consequently, even if the degree of misfocus were known, different digital filters would be required for different portions of the image, and parts of the spatial-frequency spectrum would be missing in the image, because of the zeros in the MTF. A related problem is that noise is increased greatly where the MTF has low values. However, as also shown in Fig. 5, the MTF of the system that is wave-front coded changes little over a large region of what normally is misfocus. Because the OTF has no nulls, the signal processing is not equivalent to a division by zero. After the signal processing, the PSFs of Figs. 3(C) and 3(D) appear as shown in Figs. 6(A) and 6(B). The issues of noise amplification by digital filtering, or noise gain, resulting from the sag in the MTF for the wave-front-coding system, are discussed in Section 4.

Figure 4 illustrates the use of the full increase in depth of focus to increase the depth of field. The increase in the depth of focus can be used in other ways, however. It is convenient to think in terms of

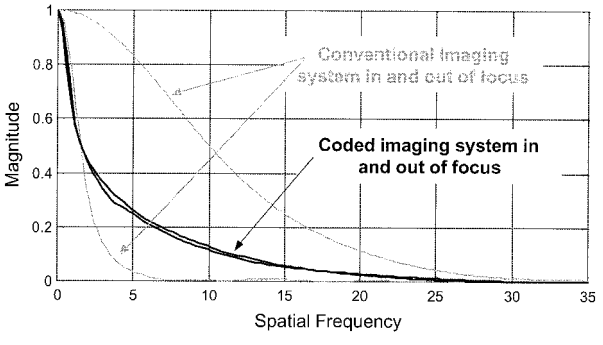

Fig. 5. MTFs corresponding with the PSFs of Fig. 3 for a conventional image in and out of focus and a coded image for the same misfocus values.

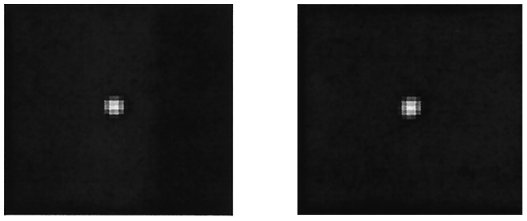

Fig. 6. PSFs after filtering. The wave-front-coded PSFs of Figs. 3(C) and 3(D), after digital filtering with a single digital filter, are shown in (A) and (B). The in-focus filtered PSF is given in (A). The greatly out-of-focus PSF is given in (B). These two PSFs are essentially the same and nearly identical to the in-focus PSF from the traditional imaging system shown in Fig. 3(A).

a focus budget, which can be allocated for several uses. If the optical system is of high quality, then the entire focus budget can be used to increase the depth of field. A portion, or all, of the focus budget can be used to make the imaging system invariant to focus-related aberrations. For example, with a lens that has significant amounts of Petzval curvature or curvature of field, the image focuses on a curved surface, not on a plane. If the depth of focus is extended, then instead of a thin curved region of focus, there is a thick curved region of focus that allows a flat detector array to be used. Consequently, the imaging system is insensitive to Petzval curvature. See Fig. 7, which shows a flat CCD array in the curved region of extended focus. In a similar manner, the imaging system can be made to be insensitive to astigmatism, and chromatic aberration. Figure 8 shows that with chromatic aberration, different colors focus in different locations. When the depth of focus is extended, there is a region where the foci for each color overlap, thereby making the imaging system invariant to chromatic aberration. Figure 9 shows images of the center section of a U.S. Air Force resolution chart. One set of images was formed with a conventional system composed of two singlets made of the same optical material. This was done to provide an image system with severe chromatic aberration but well-controlled monochromatic aberrations. The second set of images was formed with that same set of two singlets but with a phase plate having the shape of Fig. 1 between the two lenses.[7]

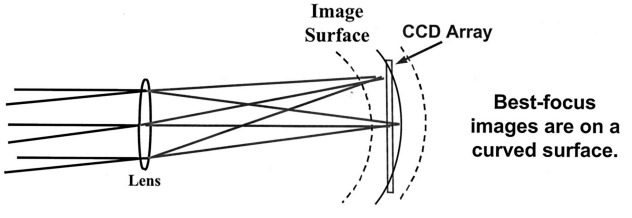

Fig. 7. Using depth of focus to control effects of field curvature. Images are formed on curved surfaces with field curvature. When a large depth of focus is available, the detector plane can fit within the extended depth of focus volume. All parts of the image within this volume will image clearly.

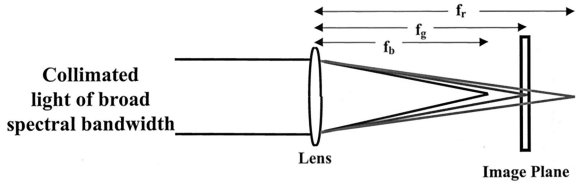

Fig. 8. Using depth of focus to control axial chromatic aberration. With small depth of focus only a small region of the spectrum is imaged clearly. Other colors form blurred images. With a large depth of focus all colors can form clear sharp images.

These examples illustrate that an imaging system with an extended depth of focus can be thought of as having a large focus budget, which can be applied to extending the depth of field (in the object domain) or to any focus-related aberrations. Also, the focus budget can be allocated for several uses.

Before discussing the trade-offs that are made in the design of a system that uses wave-front coding, and showing some interesting examples of images that can be obtained in such systems, we discuss some of the tools that are used to analyze and design these systems.

3. Theory of Wave-Front Coding

Wave-front coding modifies the optics in such a manner as to preserve some aspects of the image that is being formed. The signal processing to decode the image that is formed by the detector array (the intermediate image) is determined by the coding that is impressed on the wave front. The term signal processing also includes the spatial integration provided by the width, height, and spacing of the pixels. Hence the final image in a system with wave-front coding is a result of the optics that codes the wave front and the signal processing that decodes the intermediate image to form the final image.

A. Woodward Function

In this subsection we discuss the Woodward function as used in the analysis and design of hybrid imaging systems. P. M. Woodward showed that the capability of a radar system to determine both the range and the velocity of a target can be shown by a mathematical function that became known as the ambiguity function.[8] The ambiguity function shows how well systems can trade off accuracy in measurements of transit time of the pulse (range to the target) and in the Doppler shift in the frequency of the returned pulse (velocity of the target). Brenner *et al*. showed that the ambiguity function, with differently defined variables, can be used to represent the OTF of an imaging system.[9]

The ambiguity function for a radar signal is

$$A(u, v) = \int P(x + u/2)P^*(x - u/2)\exp(\mathrm{j}2\nu x)\mathrm{d}x, \tag{2}$$

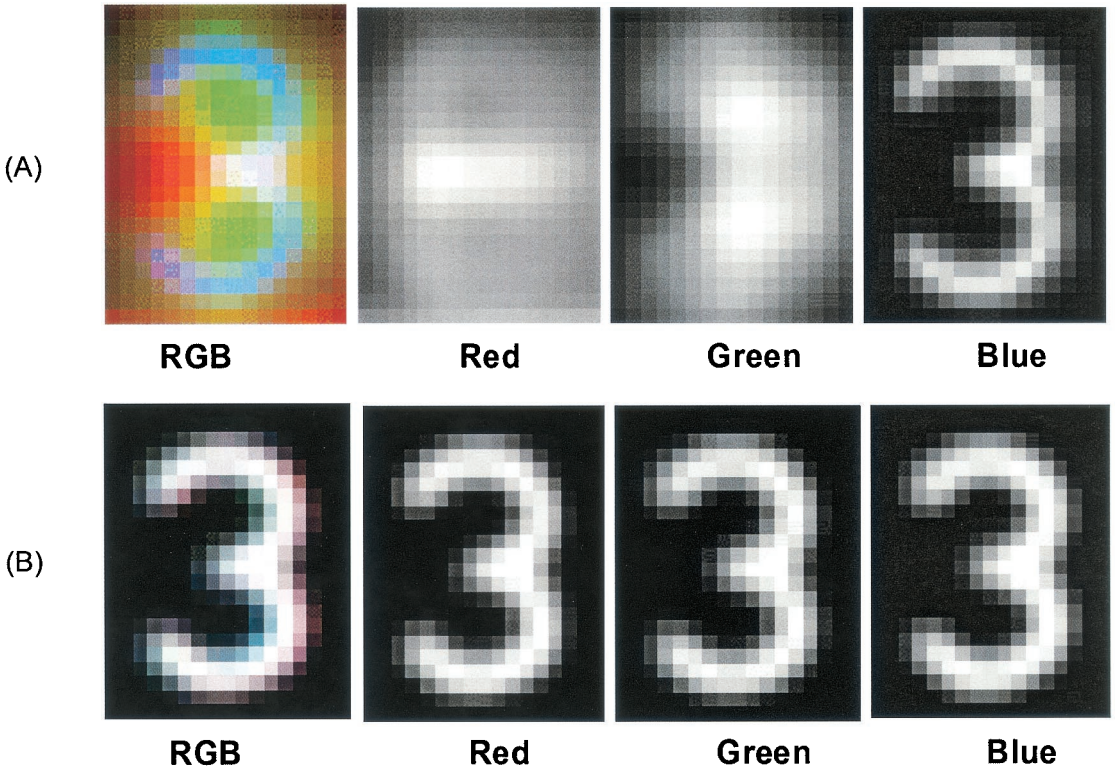

Fig. 9. Example of large depth of focus to control axial chromatic aberration. The object is from a small section of a U.S. Air Force resolution target. An imaging system with a large amount of axial chromatic aberration produces badly blurred images in red and green, whereas the blue image is sharply focused. When modified with wave-front-coding optics and signal processing, the resulting images are sharp and clear in all colors, producing a black-and-white three-color image of the black and white object.

where $j = \mathrm{sqrt}(-1)$, * denotes complex conjugate, and $P(x)$ is a complex function representing the waveform that is transmitted by the radar system. The OTF of a one-dimensional imaging system for different values of misfocus, ψ, is

$$H(u, \psi) = \int \{P(x + u/2)\exp[j(x + u/2)^2\psi]\}\{P^*(x - u/2)\exp[-j(x - u/2)^2\psi]\}\mathrm{d}x, \quad (3)$$

where $P(x)$ represents the complex pupil function of the imaging system. The misfocus parameter ψ is written in terms of physical parameters as

$$\psi = [\pi L^2/(4\lambda)(1/f - 1/d_o - 1/d_i) = 2\pi W_{20}/\lambda = kW_{20}, \quad (4)$$

where L is the width of the aperture, f is the focal length of the lens, λ is the wavelength of the illumination, d_o is the distance between the object and the first principal plane of the lens, d_i is the distance between the second principal plane of the lens and the image plane, and W_{20} is the traditional misfocus aberration constant. The parameter k is the wave number. A comparison of Eqs. (2) and (3) shows that

$$H(u, \psi) = A(u, u\psi/\pi). \quad (5)$$

The mathematics of the Woodward function as used for the ambiguity function has been studied extensively for both radar[8,10] and optics.[9,11,12] One can apply the mathematical tools and mathematical properties that were worked out for the ambiguity function to the study of misfocused imaging systems. For example, the squared power under the Woodward function is a constant. As applied to imaging systems, this means that the signal power over all misfocus values is a constant. The power can be shifted about under an envelope with wave-front coding, but it cannot be increased or decreased. As applied to the OTF, the total power under a section of the Woodward function at a particular value of spatial frequency is also a constant. Consequently, there is constant total power for all misfocus values at any given spatial frequency. The total OTF power can be bunched up about the normal in-focus position as shown in Fig. 10 below, or it can be spread out as shown in Fig. 11, but the total power for that spatial frequency does not change.

B. Woodward Function Shows the Depth of Field and Trade-Offs

A display of the Woodward function for a high-quality, one-dimensional lens is shown in Fig. 10(A). The horizontal line and the slanted line represent in-focus ($\psi = 0$) and out-of-focus slices, respectively, through the Woodward function. The horizontal slice ($\psi = 0$) gives the OTF for an in-focus system.

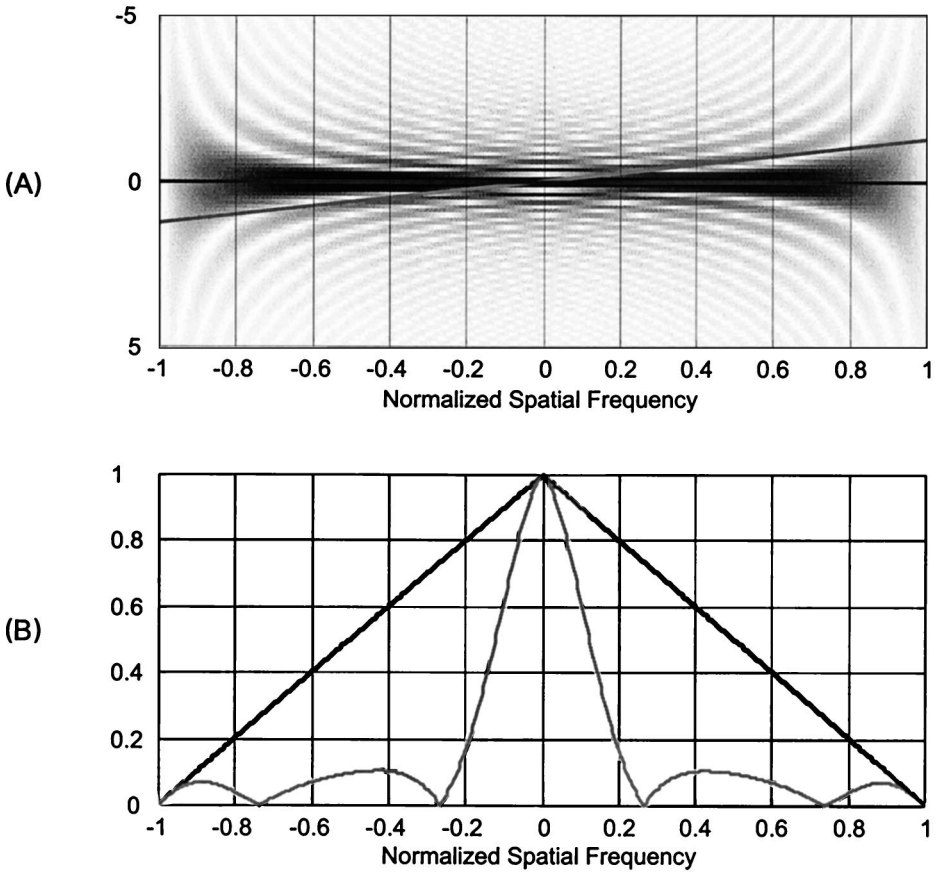

Fig. 10. Woodward function for a traditional lens with no aberrations is shown in (A). The trace through the Woodward function along the horizontal axis represents the in-focus MTF. The trace along the inclined line describes an out-of-focus MTF. Both the in-focus and the out-of-focus MTFs are shown in a traditional manner in (B).

For the out-of-focus system ($\psi \neq 0$), a slice at that angle will give a scaled OTF for that misfocus value of ψ. Projection onto the horizontal axis gives the correct scaling for the spatial frequency axis for the OTFs for misfocused systems. The magnitudes of an in-focus and an out-of-focus OTF, the MTFs, are shown in Fig. 10(B). In this case, the out-of-focus MTF goes through a zero, where there is a phase shift, giving a contrast reversal in the image.

Figure 11(A) shows the Woodward function for a one-dimensional lens with a cubic phase function, $\phi = \alpha x^3$ added in the aperture stop.[6] The change in the Woodward function clearly shows that the modified imaging system has a greater depth of field than the traditional imaging system. The energy in the spatial frequencies of the image is spread over a larger misfocus region. The slices in the Woodward function of Fig. 11 are at the same angles and hence denote the same misfocus values as in Fig. 10. Note that the MTFs of Fig. 11(B) are similar, which implies that the imaging system will have an extended depth of focus. Since the total power in the Woodward function is constant, increasing the width of the Woodward function (or increasing the depth of focus) results in lower values of the MTF compared with the traditional in-focus MTF. Furthermore, note that the MTF for the misfocused case does not go through a zero. This means that the signal processing, which is needed to restore the MTF to that of the in-focus traditional imaging system, can be done without severe increases in noise.

C. General Framework for Design

The general framework of wave-front coding allows a number of unique perspectives when considering modern optical systems. These perspectives provide designers new tools to face important challenges in the design and implementation of imaging systems. There are three main perspectives that we commonly use. These perspectives center on (1) maximizing image information, (2) increasing the degrees of freedom or system trade space, or (3) trading electronics for physical optics. Maximizing image information is often a goal for high-performance imaging systems such as microscopes. Increasing the degrees of freedom or system trade space is often a goal for IR or space-based imaging systems in which significant difficulties arise from thermal and mechanical instability. Trading electronics for physical optics is important in imaging systems that are produced in large quantities, in which maximum reduction of the cost to produce the systems is important.

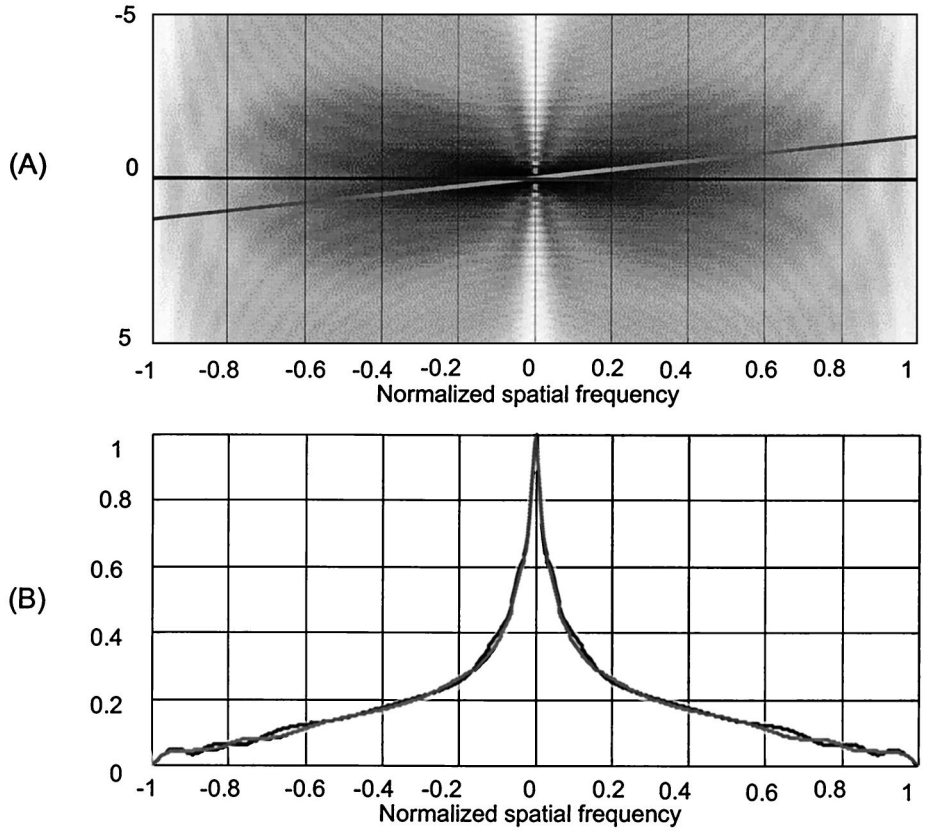

Fig. 11. Woodward function for a one-dimensional lens modified by a cubic phase function, $\phi = \alpha x^3$, is shown in (A). The optical power represented in the Woodward function for the cubic phase system is much broader than that of the traditional system. Traces of optical power through this Woodward function through the horizontal axis and at an inclined angle are displayed in the traditional manner in (B). The MTFs differ little with misfocus, in contrast to those of the traditional system of Fig. 10.

D. Maximize Image Information

In high-performance imaging systems nearly all aspects of the system that could reduce image quality are carefully controlled. In microscopes, for example, the illumination, optics, and mechanical and thermal stability are often of the highest quality and produce near-diffraction-limited images. By modifying the optics and using signal processing, the total amount of image information that can be recorded over a volume can be increased. For a number of applications this increase in information can allow a single image to be used where a number of images taken at different object planes had been used before. Reducing the number of images required can increase frame rates, reduce bleaching of fluorescent objects, and reduce overall system costs.

Image information is maximized with wave-front coding systems by means of capturing image information from a much larger object volume than is possible with traditional imaging systems. Consider imaging an object volume that is large compared with the depth of field of a traditional imaging system. Only a small region of this volume can be imaged clearly. Outside the depth of field of the imaging system, the objects are out of focus and are imaged with a large blur. The MTFs of traditional imaging systems when out of focus have regions of nulls and also act as spatial low-pass filters. The low-pass nature of traditional out-of-focus optics destroys image information. Because information is never increased by signal processing, only potentially destroyed, no amount of signal processing can restore the lost image information.

When the traditional imaging system is modified with wave-front coding, there are no nulls in the MTFs for both geometrically in-focus and out-of-focus images. The absence of these nulls means that the amount of image information that can be captured is now spread over a much larger volume of the object space. The coded optics produce no spatial-frequency nulls but have a lower transfer function than a traditional in-focus MTF. This is the image information trade-off. Making the imaging system less sensitive to misfocus allows image information to be captured over a much larger region than otherwise would be possible. But less information density compared with that of a traditional system is captured from any one narrow region in object space, because of the lowered MTF.

Mathematical measures of image information that have been applied to wave-front coding include Fisher Information[13] and Shannon Information.[14]

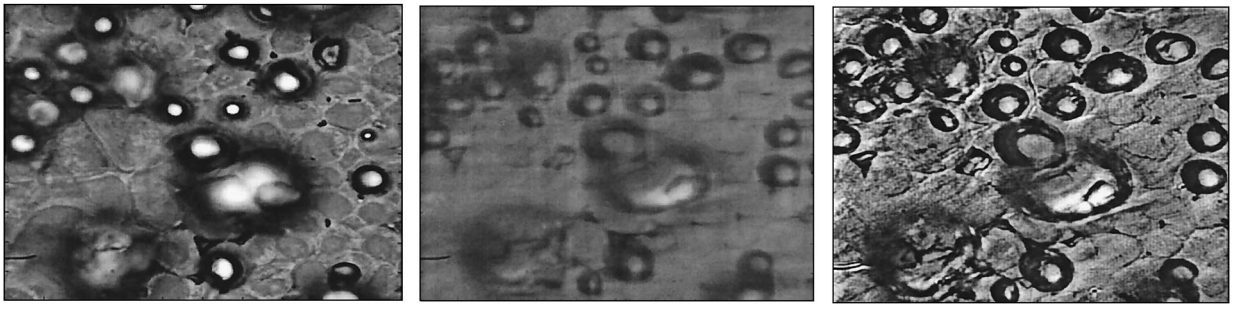

Fig. 12. Image information in traditional versus wave-front-coded images with magnification of 100× and NA of 1.3. A traditional image of a leaf with oil bubbles is given in (A). The leaf occupies a small volume relative to the oil bubbles. The bubbles are so large that all are poorly imaged, and a number in the upper right-hand corner are not imaged at all. After the optics are modified with a simple cubic phase element, the image of (B) results. Note that all parts of the image are blurred equally. Even with the blur, many aspects of the object are recognizable. Note that objects in the upper right-hand corner are clearly visible in this image, whereas they were not imaged at all with the traditional system. After signal processing, the image of (C) is formed. The objects are sharp and clear. The depth of field is so large that perspective distortion is apparent.

Shannon Information and the properties of the Woodward function can be used to show that the total information captured with a wave-front-coded imaging system can be increased over a traditional imaging system. At any one spatial frequency the MTF as a function of misfocus is given by the Woodward function. The information content (or channel capacity) of this spatial frequency can be described by Shannon Information. The total information is then the integral of the Shannon Information over all misfocus and spatial frequency.

As an example we show the increase of total information possible at one spatial frequency. The Shannon Information at this one spatial frequency and object location or misfocus value is proportional to

$$\log[1 + |H(u, \psi)/\sigma|^2], \tag{6}$$

where σ^2 is the additive rms noise power. Here we assume that the additive noise has a constant rms value over all values of misfocus. From Figs. 10 and 11 the values of the Woodward function and corresponding MTFs are lower for the wave-front-coded system than for the traditional system. Assume that the MTFs at one spatial frequency for all values of misfocus (essentially a vertical slice of the Woodward function) can be approximated by a constant nonzero value near the best focus and zero elsewhere. The height of this constant MTF can be related to the width (amount of misfocus tolerance) by the constant power property of the Woodward function. If the MTF height for the traditional system at a particular spatial frequency has a value of S_o and width W_o, then by the constant power properties of the Woodward function, another system that has M times larger depth of focus has a corresponding Woodward function with width $M*W_o$ and must have an MTF height of $S_o/\mathrm{sqrt}(M)$. The total amount of information that can be captured by the traditional system at this spatial frequency is then proportional to

$$W_o \log[1 + (S_o/\sigma)^2] = W_o \log(1 + \mathrm{SNR}_o), \tag{7}$$

where SNR is signal-to-noise ratio. The total amount of information that can be captured at this spatial frequency for the extended depth-of-focus system is then proportional to

$$MW_o \log\{1 + [S_o/\mathrm{sqrt}(M)\sigma]^2\} = MW_o \times \log(1 + \mathrm{SNR}_o/M). \tag{8}$$

The total information at this spatial frequency is increased in the extended depth-of-focus system if

$$\mathrm{SNR}_o \gg M, \tag{9}$$

with the total increase of information bounded by the factor M. Note that if the SNR for the wave-front-coded system is small enough, the total information can actually decrease, compared with the traditional system, when we attempt to increase the depth of focus.

An intuitive measure of increased image information with wave-front coding can be seen from Fig. 12. The object in Fig. 12 is a leaf with oil bubbles imaged at 100× with numerical aperture (NA) of 1.3. At this NA the depth of field of the imaging system is small compared with the object volume. The image from the traditional system is given in Fig. 12(A). Note that whereas the plane of the leaf is clearly imaged, the details from the bubbles are all badly blurred. After the optics for wave-front coding are modified, the image of Fig. 12(B) results. Note that all parts of this image appear to have a uniform blur. Details that were not even apparent in the traditional image can be seen in this blurred image. Particularly note the upper right-hand corner of the images where the wave-front-coding image shows many details that are completely missing from the traditional image. After signal processing, the final image Fig. 12(C) results. Note that all parts of the image are now sharp and clear. The surface of the leaf and the bubbles are all clearly imaged. The bubbles in the upper right-hand corner are clearly resolved in the

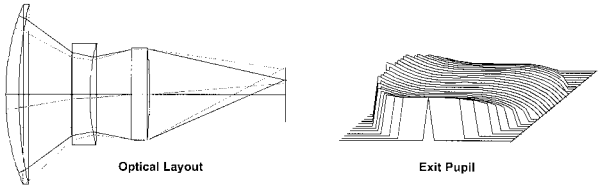

Fig. 13. IR imaging system. The fast optics, wide operating temperature, simple aluminum mounts, and lack of active thermal compensation make this a challenging design. The specifications are impossible to meet with traditional optics.

wave-front-coded image but were not resolved at all in the traditional image.

E. Increase the Degrees of Freedom or the Trade Space

IR and space-based imaging systems are examples of the types of systems that can benefit from the perspective of increased degrees of freedom or increased size of the trade space.[15] Many of these types of systems experience dynamic instabilities that are due to thermal and/or mechanical variations of the system.[14] Adequate control of the systems can generally be performed by a variety of optical and mechanical means, although for many applications the flexibility of the systems in terms of size, weight, or cost can be severely compromised.[16,17] Increasing the number of methods that can be used to control the systems increases the degrees of freedom of the system or the size of the trade space. Increasing the degrees of freedom or size of the trade space can allow the designer added flexibility in order to minimize the size, weight, and cost of the system.[18]

One of the more difficult aspects of IR imaging systems is that the common IR optical materials have large changes in index of refraction with temperature. For example, the value of dn/dT for germanium is over 100 times that of common optical glasses. This large change in index with temperature makes it difficult to design and fabricate a simple system that works reliably over even a relatively small temperature range. Many schemes have been developed to reduce the effect of temperature changes on IR optical systems. These include using different optical materials with refractive optics,[16,17] using optical mounting materials that change with temperature such as to counteract the changes in optical properties, or using diffractive optics.[19] Wave-front coding can be used in combination with these traditional athermalization techniques to reduce the amount of traditional athermalization required. Or, with a fixed amount of athermalization, wave-front coding can be used to extend the usable temperature range of the system.

An extreme example of using wave-front coding to extend the usable temperature range of an uncooled IR imaging system with no athermalization is shown in Fig. 13. The design goals for this system were an $F/2$ system with a 100-mm focal length and a $\pm 3°$ half field of view. The operating wavelength was 10 μm, and the pixel size was 20 μm. The first and third optical elements were made of silicon, and the second of germanium. The mounts were of aluminum, and the temperature range was -20 to $+70$ °C with no thermal compensation. The fast speed, simple aluminum mounts, wide operating temperature, and lack of thermal compensation make this design impossible to achieve with traditional optics. There are not enough degrees of freedom or suitable trade space in the optical designer's toolbox that would allow a design of such a system by traditional means. However, by use of nontraditional optics and signal processing, the degrees of freedom of the problem have greatly expanded, and all design goals can be simultaneously achieved. Instead of using sophisticated mounting arrangements that compensate for optical changes with temperature, or active thermal stabilization, relatively simple changes in the forms of the optical surfaces alone can be used to achieve good-quality imaging over a large temperature range.

Figure 14 shows the MTFs as a function of temperature for the traditional and wave-front-coded version of the IR imaging system. At a nominal temperature the traditional imaging system achieves

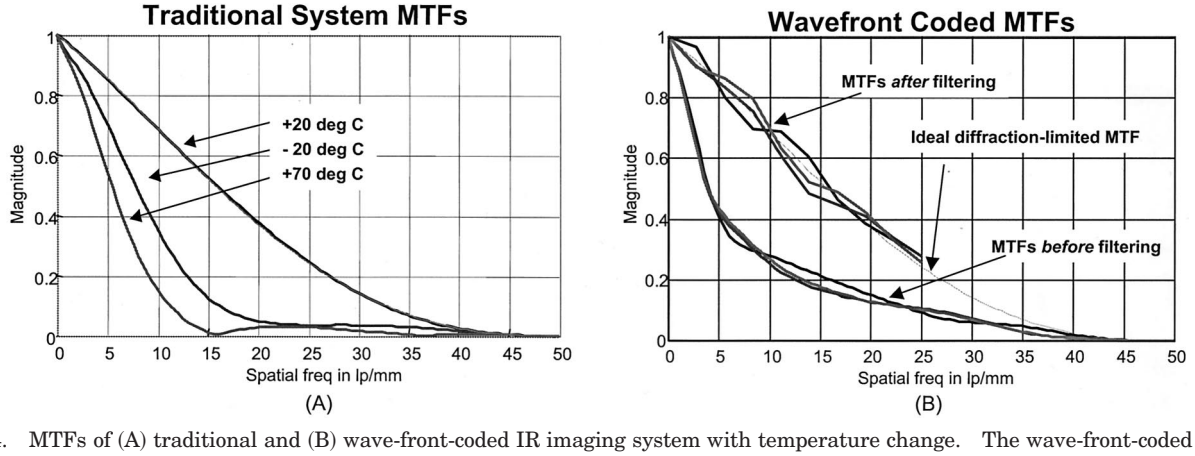

Fig. 14. MTFs of (A) traditional and (B) wave-front-coded IR imaging system with temperature change. The wave-front-coded MTFs, over the same temperature range as the traditional system, are nearly identical. After signal processing, the MTFs within the passband of the digital detector closely match the ideal diffraction-limited MTF. MTFs include pixel MTFs.

near-diffraction-limited image quality. With temperature change as slight as 10 °C, the system becomes degraded. With temperature changes in the range of 30–40 °C, the system becomes badly misfocused. When the optics are modified to become insensitive to temperature-related changes, the MTFs with temperature can be essentially constant. After filtering, the MTFs closely match the diffraction-limited performance over a 70 °C temperature range. Of course, some signal processing could be used without wave-front coding. A thermometer could indeed give one the temperature and an idea of which PSF to use in signal processing, but the MTF associated with that PSF may have zeros. The signal-processing system would have to have stored all the PSFs for a large temperature range. In addition, the PSFs would also be dependent upon the field angle, which would require space-dependent processing.

F. Trading Electronics for Physical Optical Components

The success of many consumer products, such as miniature cameras, is directly related to their cost. As the cost to produce a good-quality miniature camera decreases, economics dictates that the number of units sold increases. By use of nontraditional optics and signal processing, the physical parts costs can decrease as well as the fabrication and assembly costs.

Major challenges in the traditional design of miniature optics are fast optics with good optical quality over a large field of view and low sensitivity to fabrication and assembly errors. Because of unavoidable field curvature, fast optics that image over a large field of view often require more than one optical element for good-quality imaging. The use of more than one optical element increases the fabrication cost and assembly time. Assembly tolerances are often required to be tighter in multielement imaging systems than in single-element designs. By use of nontraditional design methods, aspheric optics and signal processing can be used to reduce the number of optical elements required and can also reduce the sensitivity of the overall system to fabrication and assembly errors. Overall costs are reduced by means of minimizing component count and minimizing fabrication and assembly time and tolerance. In these modern systems, physical quantities such as optical elements and assembly time are then traded for electronics required for the signal processing. For low-volume applications, the cost and complexity of the required electronics can exceed the cost savings in physical quantities. For other applications, particularly those with large unit volumes allowing custom electronics, the cost of the electronics can be much less than the savings made possible. Owing to the decreasing cost of electronics over time, high-volume applications will continue to favor increased electronics over quantities of optical parts and assembly time.

An example of trading electronics for physical optics is shown in Figs. 15–17. The example system is a fast single-lens imaging system with a wide field of view. The goals for this design were an $F/2.8$ system, a $\pm 25°$ field of view with a single plastic element, and a focal length of 3.5 mm. The system had to be in focus from infinity to 0.5 m. The detector pixels were 10 μm square.

A drawing of this lens system is given in Fig. 15.

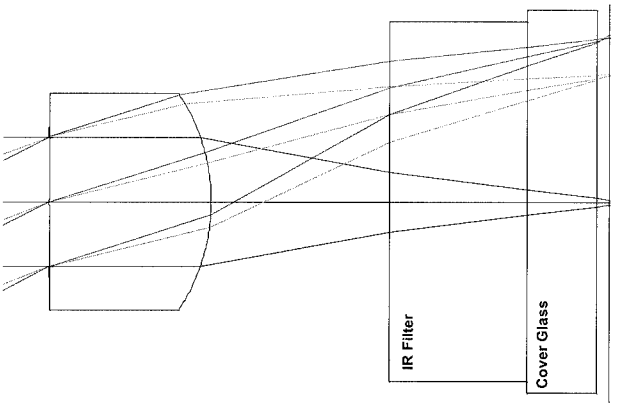

Fig. 15. Fast wide-field-of-view miniature imaging system with a single lens.

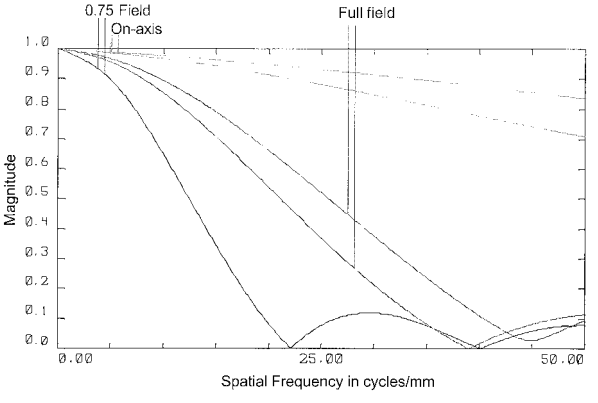

Fig. 16. Traditional single-lens imaging systems experiences large aberrations with field angle. On-axis imaging has high MTFs, but off-axis imaging is badly degraded.

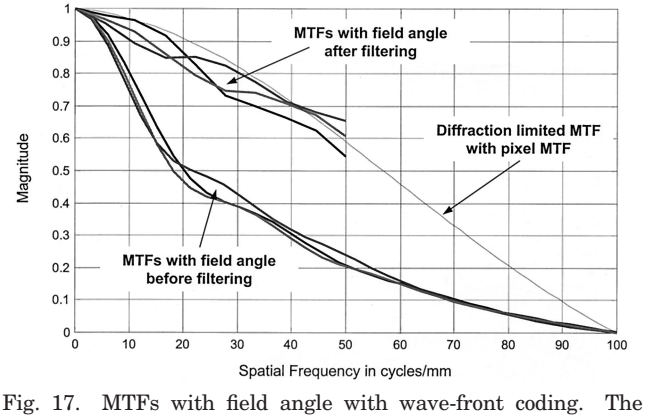

Fig. 17. MTFs with field angle with wave-front coding. The MTFs even before filtering are essentially constant over the image field. After filtering, the MTFs are similar to the diffraction-limited MTF over the spatial passband of the 10-μm pixel detector. All MTFs include the detector pixel MTFs.

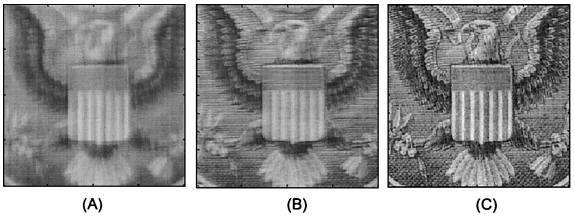

Fig. 18. Rectangularly separable filtering of gray-scale images. Image (A) is the intermediate image after wave-front-coded optics but before digital processing. Image (B) is the intermediate image after filtering each column with a one-dimensional column filter. Note that this image has vertical resolution but little horizontal resolution. Image (C) is the resulting image after filtering with both a one-dimensional column and one-dimensional row filters.

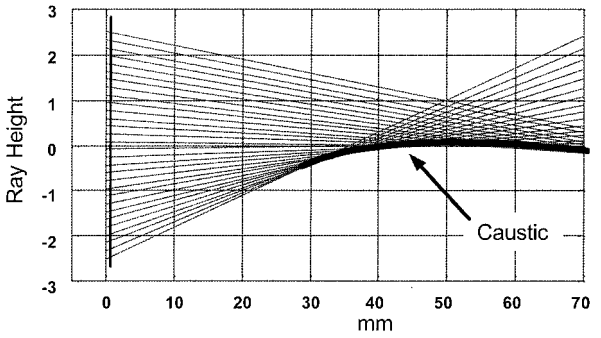

Fig. 19. Exaggerated representation of caustic in rectangularly separable cubic wave-front-coded imaging systems. During imaging, the caustic represents the movement of the centroid of the PSF with misfocus.

Figure 16 describes the MTFs of an optimized system without wave-front coding but using aspheric surfaces. The design was done with Zemax. Unavoidable field curvature aberrations cause large degradations in performance in the system over the field. Misfocus was used for partially correcting the maximum off-axis aberrations.

Figure 17 describes the MTFs of the same system but with wave-front coding. The MTFs before filtering for the system with wave-front coding are seen to be essentially constant with misfocus. After filtering, the MTFs are still essentially constant with misfocus, and are close to the diffraction-limited MTF over the passband of the digital detector.

4. Trade-Offs in Design and Performance

There are an infinite number of different phase plates that can be used to extend the depth of field. Some can be written in terms of separable mathematical functions and lead to separable signal processing. Others cannot be written in terms of separable functions and require nonseparable signal processing. For example, the phase plate that is described by

$$z = \alpha(x^3 + y^3) \tag{1}$$

leads to signal processing that is rectangularly separable. In that case, an image can be processed in two sets of one-dimensional operations allowing fast processing. Figure 18 describes rectangularly separable processing. One performs rectangularly separable processing by first filtering in the row (or column) direction with a one-dimensional row (or column) filter. Each row (or column) is independently filtered, and a temporary image is formed. Next, each column (or row) of the temporary image is filtered with a one-dimensional column (or row) filter to produce the final image. A phase plate that is described by a nonseparable function must be processed with two-dimensional kernels. Nonseparable processing requires approximately the square of the processing required for rectangularly separable processing. Nonseparable processing can be required even when a rectangularly separable phase plate is used. In this case a nonseparable distribution in the aperture of the system can be caused by aberrations that are nonseparable, such as coma. Some functions are separable in cylindrical coordinates, but the sampling is in rectangular coordinates. Consequently, rectangularly separable functions are of particular interest when fast processing of the intermediate image is desired.

Each type of phase plate has an operating range over which there is an extended depth of field. In Eq. (1) repeated above, which describes a simple cubic phase system, this range is determined by the value of α. When the design range is exceeded, the final image, which is obtained after signal processing, changes in some fashion. With a rectangularly separable cubic phase plate, the rays move in a fashion as shown in Fig. 19. One apparent change in the ray trace as the image plane is moved is that, as the caustic shows, a lateral movement of the PSF occurs. Hence, for this particular phase plate, as the operation of the imaging system exceeds the design depth of field (the region where the caustic is essentially flat), the first noticeable effect is a movement of the portions of the object in that extreme region. It also is apparent that the upper edge of the PSF is changing. Consequently, there are also small changes in the appearance of the image. These, however, are barely perceptible in comparison with the shift in the image position. Other phase plates, such as one with a phase deviation of $z = \alpha\rho^3 \cos 3\theta$, have no lateral movement of the PSF.

The MTF that is shown in Fig. 5 shows that, even though the signal level changes little over the range of misfocus, the MTF is lower over the entire range of misfocus than the level of the MTF for a conventional imaging system in focus. This sag in the MTF represents a loss of SNR. The degree of the loss in SNR depends on the amount of sag, which is proportional to the design depth of field. A metric that describes this reduced SNR in terms of the digital filter is called the noise gain. The noise gain describes the expected rms value of the noise after filtering divided by the rms value of the noise before filtering. When the

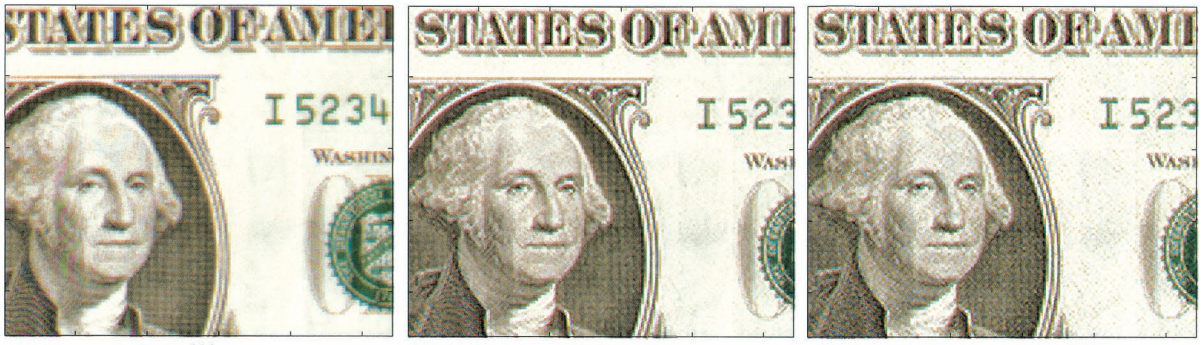

Fig. 20. Example of filtered images and additive noise. Image (A) is a Bayer-detected three-color image made with a traditional system. The object was essentially perpendicular to the optical axis. Because of aberrations, the conventional image (A) has a soft blur. Note color aliasing of the left-hand side of George Washington in the conventional image. Image (B) is a wave-front-coded version of the same image that was time averaged to minimize additive noise. Note increased spatial resolution and reduction of color aliasing. Image (C) is a nonaveraged wave-front-coded image. The digital filter had a noise gain of approximately 5.

sum of all filtering coefficients equals unity, the noise gain of the digital filter is given by the root of the summed squares of the filter coefficients.

Whether the noise appears in the image depends on several factors. One factor is the exact shape of the phase plate; different phase plates that provide the same extension of the depth of field can have different noise gains. For example, the noise gain of the separable digital filter that was used in the system of Fig. 15 had a value of 1.8, or less than 1 bit. Another factor is the dynamic range of the detector. For example, if an 8-bit detector is used with a system with a moderate increase in the depth of field, then there will be detectable noise in the image. If the detector uses 10 bits or more, then when the top 8 bits are displayed, there is little noticeable noise for even large extensions of the depth of field. Figure 20 shows images that were taken with an 8-bit camera and is useful in showing the effects of different noise levels. The image from a conventional system shows a soft blur resulting from aberrations in the imaging system. Note that color aliasing is seen in areas of the image that should contain only shades of gray. An extended depth-of-field imaging system was used to produce the images of 20(B) and 20(C). These images have higher resolution, since some of the lens aberrations have been implicitly corrected. Note also that color aliasing has also been reduced. The image of Fig. 20(B) was formed with 25 time-averaged images. Figure 20(C) shows a single image and hence has approximately five times lower SNR. Careful examination of the image of 20(C) shows the effects of the higher noise level. The digital filter used had a noise gain of 5 on account of the particular system and extension of the depth of field. A filter that produced lower contrast similar to that of the conventional image would have a lower noise gain. Although not shown, phase plates that are custom designed for particular optics or amounts of depth of field can result in much lower noise gains and additive noise after processing than systems that use a simple cubic phase plate. Systems with detectors with even more dynamic range and/or displays with less would also help with essentially removing the visual effect of additive noise.

5. Conclusion

We have described a new paradigm for designing imaging systems. This paradigm requires that the optical and signal-processing portions of the system be designed jointly. This enables the design of imaging systems that have previously unobtainable performance. Examples given involved the extension of the depth of focus of an imaging system, and that depth of focus can be used to extend the depth of field of the system and/or to make the imaging system invariant to focus-related aberrations. Images were shown of a microscope with a depth of field ten times greater. To illustrate invariance to focus-related aberrations, a single-lens imaging system and an IR system were described that used the new paradigm to perform aberration balancing.

This material is based in part upon research supported by the U.S. Army Research Office under contract/grant DAAD 19-00-1-0514.

References

1. W. T. Cathey, B. R. Frieden, W. T. Rhodes, and C. K. Rushforth, "Image gathering and processing for enhanced resolution," J. Opt. Soc. Am. A **1,** 241–249 (1984).
2. J. Ojeda-Castañeda, E. Tepichin, and A. Diaz, "Arbitrary high focal depth with quasioptimum real and positive transmittance apodizer," Appl. Opt. **28,** 2666–2670 (1989).
3. G. Häusler, "A method to increase the depth of focus by two step image processing," Opt. Commun. **6,** 38–42 (1972).
4. E. R. Dowski and W. T. Cathey, "Single-lens, single-image, incoherent passive ranging systems," Appl. Opt. **33,** 6762–6773 (1994).
5. G. E. Johnson, "Passive ranging systems using orthogonal encoding," Ph.D. dissertation (University of Colorado Boulder, Colo., 2000).
6. E. R. Dowski, Jr., and W. T. Cathey, "Extended depth of field through wave-front coding," Appl. Opt. **34,** 1859–1866 (1995).

7. H. B. Wach, E. R. Dowski, and W. T. Cathey, "Control of chromatic focal shift through wave-front coding," Appl. Opt. **37,** 5359–5367 (1998).
8. P. M. Woodward, *Probability and Information Theory with Applications to Radar* (Pergamon, New York, 1953).
9. K.-H. Brenner, A. Lohmann, and J. Ojeda-Castañeda, "The ambiguity function as a polar display of the OTF," Opt. Commun. **44,** 323–326 (1983).
10. A. W. Rihaczek, *Principles of High Resolution Radar* (McGraw-Hill, New York, 1969).
11. A. Papoulis, "Ambiguity function in fourier optics," J. Opt. Soc. Am. **64,** 779–788 (1974).
12. A. R. FitzGerrell, E. R. Dowski, and W. T. Cathey, "Defocus transfer function for circularly symmetric pupils," Appl. Opt. **36,** 5796–5804 (1997).
13. E. R. Dowski, "An information theory approach to incoherent information processing systems," in *Signal Recovery and Synthesis*, Vol. 11 of 1995 OSA Technical Digest Series (Optical Society of America, Washington, D.C., 1995), pp. 106–108.
14. J. van der Gracht and G. W. Euliss, "Information-optimized extended depth-of-field imaging systems," in *Visual Information Processing X*, S. K. Park, Z. Rahman, and R. A. Schowengerdt, eds., Proc. SPIE **4388,** 103–112 (2001).
15. M. Roberts, "Athermalization of infrared optics: a review," in *Recent Trends in Optical Systems Design and Computer Lens Design Workshop II*, R. E. Fischer and R. C. Juergens, eds., Proc. SPIE **1049,** 72–81 (1989).
16. T. H. Jamieson, "Thermal effects in optical systems," Opt. Eng. **20,** 156–160 (1981).
17. D. S. Grey, "Athermalization of optical systems," J. Opt. Soc. Am. **38,** 542–546 (1948).
18. E. R. Dowski, R. H. Cormack, and S. D. Sarama, "Wavefront coding: jointly optimized optical and digital imaging systems," in *Visual Information Processing IX*, S. K. Park and Z. Rahman, eds., Proc. SPIE **4041,** 114–120 (2000).
19. G. P. Berhmann and J. P. Bowen, "Influence of temperature on diffractive lens performance," Appl. Opt. **32,** 2483–2489 (1993).